Drug transporters and blood–testis barrier function

Linlin Su, Dolores D Mruk, Will M Lee[1] and C Yan Cheng

The Mary M. Wohlford Laboratory for Male Contraceptive Research, Center for Biomedical Research, Population Council, 1230 York Avenue, New York, New York 10065, USA

[1]School of Biological Sciences, The University of Hong Kong, Hong Kong, China

(Correspondence should be addressed to C Y Cheng; Email: y-cheng@popcbr.rockefeller.edu)

Abstract

The blood–testis barrier (BTB) creates an immunological barrier that segregates the seminiferous epithelium into the basal and apical compartment. Thus, meiosis I/II and post-meiotic germ cell development take place in a specialized microenvironment in the apical compartment behind the BTB and these events are being shielded from the host immune system. If unwanted drugs and/or chemicals enter the apical compartment from the microvessels in the interstitium via the basal compartment, efflux pumps (e.g. P-glycoprotein) located in Sertoli cells and/or spermatids can actively transport these molecules out of the apical compartment. However, the mechanism(s) by which influx pumps regulate the entry of drugs/chemicals into the apical compartment is not known. In this study, a solute carrier (SLC) transporter organic anion transporting polypeptide 3 (Oatp3, *Slco1a5*) was shown to be an integrated component of the N-cadherin-based adhesion complex at the BTB. However, a knockdown of Oatp3 alone or in combination with three other major Sertoli cell drug influx pumps, namely *Slc22a5*, *Slco6b1*, and *Slco6c1*, by RNAi using corresponding specific siRNA duplexes failed to perturb the Sertoli cell tight junction (TJ) permeability barrier function. Yet, the transport of [^{3}H]adjudin, a potential male contraceptive that is considered a toxicant to spermatogenesis, across the BTB was impeded following the knockdown of either Oatp3 or all the four SLC transporters. In short, even though drug transporters (e.g. influx pumps) are integrated components of the adhesion protein complexes at the BTB, they are not involved in regulating the Sertoli cell TJ permeability barrier function, instead they are only involved in the transport of drugs, such as adjudin, across the immunological barrier at the BTB.

Journal of Endocrinology (2011) **209,** 337–351

Introduction

The blood–testis barrier (BTB) created by adjacent Sertoli cells near the basement membrane in the seminiferous epithelium of the testis maintains one of the tightest barrier-tissue barriers in the mammalian body, which segregates the entire events of i) meiosis I and meiosis II and ii) post-meiotic spermatid development, namely spermiogenesis and spermiation, from the systemic circulation (Cheng & Mruk 2002, 2010, O'Donnell *et al.* 2011). Thus, developing germ cells must rely on Sertoli cells for structural and nutritional support in the seminiferous epithelium (Mruk *et al.* 2008). The BTB also imposes an immunological barrier to prevent unwanted and harmful substances from reaching the microenvironment in the apical compartment restricted for spermatid development and by shielding meiotic and haploid germ cells from being recognized and attacked by the host immune system because many specific antigens are expressed transiently in these developing germ cells (Mruk *et al.* 2008, Cheng & Mruk 2010, Cheng *et al.* 2011). Additionally, the BTB plays an important role to confer the testis the immune-privileged status (Meinhardt & Hedger 2010). However, this unique barrier also creates a major hurdle in drug development for male contraception and treatment of testicular cancer (e.g. germ cell tumors) if these drugs exert their effects behind the BTB (Mruk & Cheng 2008). Thus, there is much interest to investigate the role of drug transporters, such as efflux pumps (e.g. P-glycoprotein) and influx pumps (e.g. organic anion transporting polypeptides (Oatps, including Oatp1, Oatp2, Oatp3 (*Slco1a5*), and Oatp4), which are members of a solute carrier (SLC) transporter subfamily), in regulating drug trafficking across blood–tissue barriers, in particular, at the blood–brain barrier and the blood–retinal/ocular barrier (Dallas *et al.* 2006, Miller *et al.* 2008). Recent studies have identified several drug transporters in the testis (Suzuki *et al.* 2003, Augustine *et al.* 2005, Su *et al.* 2009). For instance, P-glycoprotein was shown to be an integrated component of the occludin-, claudin-11-, and JAM-A-based adhesion protein complexes at the BTB, and a significant but transient increase in their association was also detected when rats were treated with adjudin (1-(2,4-dichlorobenzyl)-*1H*-indazole-3-carbohydrazide (Su *et al.* 2009), a potential male contraceptive known to exert its effects at the Sertoli–spermatid interface by disrupting the apical ectoplasmic specialization (apical ES, a testis-specific atypical adherens junction type) anchoring device to induce

DOI: 10.1530/JOE-10-0474
0022–0795/11/0209–337
Online version via http://www.endocrinology-journals.org

spermatid loss from the seminiferous epithelium (Cheng & Mruk 2002, Mruk *et al.* 2008, Wong *et al.* 2008*a*)). We interpret that this surge in the steady-state protein level of P-glycoprotein and its increase in association with the adhesion protein complexes at the BTB (Su *et al.* 2009) are likely used by the testes to 'pump' adjudin, a toxicant to spermatogenesis, out of the apical compartment in the seminiferous epithelium to protect post-meiotic spermatid development. Thus, we sought to examine whether Oatp3 (*Slco1a5*; Meier & Stieger 2002, Klaassen & Aleksunes 2010, Su *et al.* 2010*b*, Ueno *et al.* 2010) – a widely expressed influx drug pump known to transport thyroid hormones, prostaglandin E_2, organic anions and signal mediators across the blood–brain barrier (Abe *et al.* 1998, Ohtsuki *et al.* 2004) and bile acid across the gut barrier in intestine (Cattori *et al.* 2001) and is found in the testis (Augustine *et al.* 2005, Su *et al.* 2009) – was structurally associated with integral membrane proteins at the BTB. We also investigated whether Oatp3 (*Slco1a5* alone, or in combination with other SLC transporters (influx pumps), such as *Slc22a5* (a SLC organic cation transporter family member 5, also known as OCTN2, a Na^+-dependent organic cation/carnitine transporter 2, involved in the transport of carnitine and organic cations), *Slco6b1* (a SLC organic anion transporter family member 6b1, also known as a testis-specific transporter-1 (TST-1), or GST-1, gonad-specific transporter, implicated in Schwann cell development and involved in the transport of dehydroepiandrosterone sulfate, sex steroids and thyroid hormones), and *Slco6c1* (a SLC organic anion transporter family member 6c1, also known as TST-2 or GST-2, involved in the transport of thyroxine, taurocholic acid, and dehydroepiandrosterone), which are highly expressed in Sertoli cells in the testis (Collarini *et al.* 1992, Mizuno *et al.* 2003, Suzuki *et al.* 2003, Augustine *et al.* 2005, Ueno *et al.* 2010) and are known to be involved in drug transports in epithelia under normal and pathological conditions (Rochat 2009, Kis *et al.* 2010, Klaassen & Aleksunes 2010), would regulate the entry of drugs (e.g. adjudin) from the basal to the apical compartment across the BTB. We also assessed whether the entry of adjudin into the epithelium behind the BTB is mediated by changes in the Sertoli cell tight junction (TJ) permeability barrier if *Slco1a5* is a structural component of the adhesion protein complexes at the BTB.

Materials and Methods

Animals

The use of Sprague–Dawley rats in all the experiments reported in this study was approved by the Rockefeller University Animal Care and Use Committee with Protocol Numbers 06018 and 09016.

Antibodies

Antibodies were either obtained commercially or prepared in our laboratory and the appropriate working dilutions are listed in Table 1. All commercially purchased antibodies are known to cross-react with the corresponding proteins in rats as indicated by the manufacturers.

Primary Sertoli cell cultures

Primary Sertoli cells were isolated from 20-day-old rat testes and cultured in F12/DMEM supplemented with growth factors and bacitracin as described earlier (Cheng *et al.* 1986, Mruk *et al.* 2003, Su *et al.* 2009). Sertoli cells were plated on Matrigel (BD Biosciences, Bedford, MA, USA)-coated 12-well culture plates at i) $0{\cdot}5\times10^6$ cells/cm^2 for lysate preparation or for RNA extraction and ii) $0{\cdot}05\times10^6$ cells/cm^2 on coverslips for dual-labeled immunofluorescence (IF)

Table 1 Primary antibodies used for different experiments in this report

Target protein	Catalog no.	Lot no.	Host	Vendor	Usage
Oatp3	sc-47265	A1408	Goat	Santa Cruz Biotechnology	IB (1:200), IHC (1:50), IF (1:50), IP (1:40)
OatpY	sc-102045	G1608	Rabbit	Santa Cruz Biotechnology	IB (1:200)
P-glycoprotein	517310	D00087822	Mouse	Calbiochem (San Diego, CA, USA)	IB (1:300)
	sc-55510	B1108	Mouse	Santa Cruz Biotechnology	IF (1:50)
Mrp1	sc-13960	I1906	Rabbit	Santa Cruz Biotechnology	IB (1:200)
Claudin-11	36-4500	387613A	Rabbit	Zymed/Invitrogen	IB (1:250), IF (1:50)
JAM-A	36-1700	463126A	Rabbit	Zymed/Invitrogen	IB (1:250), IF (1:50)
ZO-1	61-7300	450085A	Rabbit	Zymed/Invitrogen	IB (1:250), IF (1:50)
Occludin	71-1500	636024A	Rabbit	Zymed/Invitrogen	IB (1:250), IF (1:50)
N-cadherin	sc-7939	H0907	Rabbit	Santa Cruz Biotechnology	IB (1:200), IF (1:50)
β-Catenin	71-2700	60806848C2	Rabbit	Zymed/Invitrogen	IB (1:250), IF (1:50)
FAK	06-543	31701	Rabbit	Upstate (Billerica, MA, USA)	IB (1:1000)
c-Src	sc-8056	D0408	Mouse	Santa Cruz Biotechnology	IB (1:200)
Laminin β3	–	–	Rabbit	Cheng Lab (Yan & Cheng 2006)	IF (1:75)
Laminin γ3	–	–	Rabbit	Cheng Lab (Yan & Cheng 2006)	IF (1:75)
β1-Integrin	610468	02070	Mouse	BD Biosciences	IF (1:50)
Actin	sc-1616	F0809	Goat	Santa Cruz Biotechnology	IB (1:200)

IB, immunoblotting; IHC, immunohistochemistry; IF, immunofluorescence microscopy; IP, immunoprecipitation.

analysis or plated at iii) $1{\cdot}2\times10^6$ cells/cm^2 on Matrigel-coated Millicell bicameral units to assess the Sertoli cell TJ permeability barrier by quantifying transepithelial electrical resistance (TER) across the cell epithelium and for [^{3}H]adjudin transport assay. It is noted that Sertoli cells cultured on Matrigel-coated dishes or bicameral units is known to establish a functional TJ permeability barrier (Grima *et al.* 1992, 1998, Lui *et al.* 2001) with ultrastructures of TJ, basal ES, and desmosome when examined by electron microscopy (Siu *et al.* 2005), which mimics the BTB *in vivo* (Byers *et al.* 1986, Janecki & Steinberger 1986, Mruk *et al.* 1997). This *in vitro* system has widely been used by investigators in the field to study Sertoli cell BTB regulation (Janecki *et al.* 1991*a*, 1992, Okanlawon & Dym 1996) including our laboratory (Lui *et al.* 2001, Wong *et al.* 2008*b*, Yan *et al.* 2008*b*, Siu *et al.* 2009*a*). Also, Sertoli cells isolated from 20-day-old rat testes are fully differentiated and ceased to divide (Orth 1982), and these cells are functionally indistinguishable from adult Sertoli cells isolated from adult rat testes (Li *et al.* 2001*a*, Lui *et al.* 2003*a*).

Drug transporters knockdown in Sertoli cell epithelium by RNAi

For RNAi experiments, Sertoli cells were transfected with 100 nM non-targeting control siRNA or specific *Oatp3* (*Slco1a5*) siRNA duplexes (Ambion/Applied Biosystems, Austin, TX, USA, see Table 2) for Oatp3 single knockdown; 200 nM non-targeting control duplexes, a mixture of 50 nM *Slco1a5* plus 150 nM control siRNA duplexes or a mixture of *Slco1a5*, *Slc22a5*, *Slco6b1*, and *Slco6c1* siRNA duplexes (50 nM each) in multiple influx drug transporters (MIDTs) knockdown experiments using RiboJuice siRNA Transfection Reagent (Novagen/EMD4 Biosciences, San Diego, CA, USA). The sequences of the four drug transporters' siRNA duplexes are listed in Table 2. The sequences of the non-targeting control siRNA duplexes (Silencer Select Negative Number 1 siRNA) were not available from the manufacturer (Ambion), but the Catalog number is listed in Table 2. Transfection was performed routinely on day 3 when an intact Sertoli cell epithelium with a functional TJ permeability barrier was established as described earlier (Li *et al.* 2009, Lie *et al.* 2010). About 24 h thereafter, transfection mixture was removed and replaced with fresh F12/DMEM, and cells were cultured for another 48 h before their termination. In dual-labeled IF analysis, siGLO Red Transfection Indicator (Dharmacon/Thermo Fisher Scientific, Lafayette, CO, USA) was co-transfected with specific siRNA duplexes to confirm successful transfection. Off-target effects of the silencing experiments were assessed by immunoblot analysis using multiple marker proteins at the BTB including two efflux pumps: P-glycoprotein and multidrug resistance-associated protein 1 (Mrp1).

Administration of adjudin to adult rats and in vitro *treatment of Sertoli cells with adjudin*

Adjudin (50 mg/kg b.w., suspended in 0·5% methylcellulose (wt/vol)) was administered to adult rats (≈300 g b.w.) by gavage with a single dose to induce germ cell loss from the seminiferous epithelium (Cheng *et al.* 2001, Su *et al.* 2009). Rats were killed by CO_2 asphyxiation at selected time points at 0, 3, 6, 9, and 12 h, and 1, 2 and 4 days after treatment ($n=3$–5 rats per time point), testes were removed immediately under aseptic conditions, snap-frozen in liquid nitrogen and stored at −80 °C until used. Testis lysate was obtained for immunoblot analysis as described (Su *et al.* 2010*c*). Cross-sections (7 μm thick) of testes were obtained with a cryostat at −20 °C and used for immunohistochemistry (IHC; Su *et al.* 2010*a*, Siu *et al.* 2011). For Sertoli cell cultures, adjudin (1 μg/μl stock, dissolved in ethanol) was added to F12/DMEM at a final concentration of 1 μg/ml. Sertoli cells were treated with media containing adjudin daily and terminated for dual-labeled IF analysis at specified time points.

[^{3}H]adjudin transport assay in Sertoli cell epithelium with a functional BTB that mimics the BTB in vivo

[^{3}H]adjudin [indazole-5,7-^{3}H(*N*)]-1-(2,4-dichlorobenzyl)-*1H*-indazole-3-carbohydrazide, specific activity, 580 mCi/mmol) was obtained from Perkin Elmer (Boston, MA, USA). The purity of this radiolabeled adjudin was shown to be at least 98% pure by reverse-phase HPLC using a Zorbax SB-C18 HPLC column (4·6×250 mm i.d.). Sertoli cells were cultured on Matrigel-coated bicameral units at $1{\cdot}2\times10^6$ cells/cm^2 for 3 days to form an intact epithelium with a functional TJ permeability barrier established when assessed by TER across the cell epithelium and having the

Table 2 Primers of siRNA duplexes used for RNAi experiments to knockdown different drug transporters (influx pumps)[a]

Gene	**siRNA sequence** (sense)	**siRNA sequence** (anti-sense)	**siRNA ID no.**
Oatp3 (*Slco1a5*)	5′-GCAUUGGAUAUUUACUUAUtt-3′	5′-AUAAGUAAAUAUCCAAUGCat-3′	s135280
	5′-GUAUCAAGCCUGAAGAGAAtt-3′	5′-UUCUCUUCAGGCUUGAUACac-3′	s135282
	5′-CAGCAGAGUGUAUAAAAGAtt-3′	5′-UCUUUUAUACACUCUGCUGgg-3′	s135281
Slc22a5	5′-CCUUAGGAGUUUGCAUAUUtt-3′	5′-AAUAUGCAAACUCCUAAGGtg-3′	s132113
Slco6b1	5′-GGACCACUGCUUUUUCGAAtt-3′	5′-UUCGAAAAAGCAGUGGUCCag-3′	s139506
Slco6c1	5′-CAGUUGCAAUUACGAAAUUtt-3′	5′-AAUUUCGUAAUUGCAACUGtc-3′	s142031

[a]Sequences for the non-targeting control duplexes (Silencer Select Negative Number 1 siRNA, Cat. no. 4390843) are not available from the manufacturer (Ambion).

Table 3 Primers used for RT-PCR

Gene	Primer sequence	Orientation	Position	Length (bp)	GenBank accession no.	Cycle no.	T_m (°C)
Oatp3 (*Slco1a5*)	5′-GGAGAAACAGAGAAAAGGGT-3′	Sense	4–23	175	NM_030838	25	53
	5′-ATCCAACTATAGATGTGGGG-3′	Anti-sense	178–159				
Slc22a5	5′-TGGTGTGTAAGGATGACTGGAA-3′	Sense	401–422	211	NM_019269	25	55
	5′-CCAACAAGGACAAAAAGCACT-3′	Anti-sense	591–611				
Slco6b1	5′-CATCAGAGTATTCCCTTATCA-3′	Sense	249–269	201	NM_133412	25	52
	5′-CAGAACGAGATAAGAAAGAAG-3′	Anti-sense	429–449				
Slco6c1	5′-TTTCTTCATCATTGGGCAGTGT-3′	Sense	642–663	255	NM_173338	25	54
	5′-TTCCACCACCCAAACTGC-3′	Anti-sense	879–896				

ultrastructures of TJ, basal ES, and desmosome-like junction when examined by electron microscopy as described (Siu *et al.* 2005). Thereafter, Sertoli cells were transfected with non-targeting control siRNA duplexes, *Slco1a5* siRNA duplexes, or a mixture of *Slco1a5*, *Slc22a5*, *Slco6b1*, and *Slco6c1* siRNA duplexes for quadruple knockdown. siRNA duplexes were removed 24 h thereafter, and 3 days after transfection, [^{3}H]adjudin (~$0{\cdot}6\times10^6$ c.p.m.) was added to the basal compartment of each bicameral unit. About 50 μl aliquot of F12/DMEM was withdrawn from the apical or basal compartment at selected time points: 0, 0·5, 1·5, 3, 4, 5, 6, 7, and 9 h and placed in scintillation vials together with 3 ml liquid scintillation cocktail (Beckman Coulter Inc., Brea, CA, USA) for radioactivity determination using a β-counter.

Immunoblot analysis and co-immunoprecipitation

Lysates from testes or Sertoli cells were prepared in immunoprecipitation (IP) lysis buffer (10 mM Tris, 0·15 M NaCl, 1% NP-40, and 10% glycerol, pH 7·4 at 22 °C) supplemented with protease and phosphatase inhibitor cocktails (Sigma–Aldrich) according to the manufacturer's instructions as described earlier (Su *et al.* 2009). Lysates (~100 μg protein from testes or 50 μg from Sertoli cells) were resolved by SDS-PAGE for immunoblot analysis with target proteins being probed by the corresponding primary antibodies (Table 1) as described earlier (Su *et al.* 2009, 2010*c*). Protein estimation was performed by spectrophotometry with a Bio-Rad Dc Protein Assay Kit using BSA as a standard and a Bio-Rad Model 680 Plate Reader. Co-immunoprecipitation (Co-IP) was performed to identify proteins that are structurally associated with *Slco1a5* as described (Su *et al.* 2009). In brief, 2 μg normal goat IgG was added to 300 μg lysates of Sertoli cells, incubated for an hour before precipitated with 10 μl protein A/G agarose beads (1 h), and the supernatant was obtained (1000 ***g***, 5 min). This pre-cleaning step removed non-specific interacting proteins from the cell lysates. Thereafter, lysates were incubated with 2 μg normal goat IgG as negative control or specific anti-Oapt3 antibody for Co-IP on a Labnet MiniLabRoller overnight, to be followed by incubation with 20 μl protein A/G agarose beads (Santa Cruz Biotechnology, Santa Cruz, CA, USA) to extract the immunocomplexes. Thereafter, beads were washed with IP lysis buffer and immunocomplexes (*Slco1a5* and its interacting protein partners) were extracted in an SDS-PAGE sample buffer at 100 °C for SDS-PAGE and immunoblot analysis. Sertoli cell lysate (20 μg protein) without IP served as a positive control.

IHC and dual-labeled IF analysis

IHC and dual-labeled IF analysis were performed essentially as described earlier (Wong *et al.* 2008*b*, Yan *et al.* 2008*a*, Su *et al.* 2009). Frozen sections of testes (~7 μm thick) were obtained with a cryostat and fixed with Bouin's fixative. Cultured Sertoli cells were fixed with 4% paraformaldehyde in PBS (10 mM sodium phosphate, 0·15 M NaCl, pH 7·4 at 22 °C). Primary antibodies were incubated at room temperature

Table 4 Primers used for real-time PCR (qPCR)

Gene	Primer sequence	Orientation	Position	Length (bp)	GenBank accession no.	Cycle no.	T_m (°C)
Oatp3 (*Slco1a5*)	5′-ACCTTCTGTATTTCTTGC-3′	Sense	1196–1213	88	NM_030838	40	60
	5′-GGGTGGTGAACTCCTT-3′	Anti-sense	1268–1283				
Slc22a5	5′-CGCCTTCCACTATCTTC-3′	Sense	923–939	96	NM_019269	40	60
	5′-TATTTCGTGTTCGGACC-3′	Anti-sense	1002–1018				
Slco6b1	5′-TATGGTCTGGGTTATGC-3′	Sense	949–965	97	NM_133412	40	60
	5′-ACTGCCACCAAAGAAA-3′	Anti-sense	1030–1045				
Slco6c1	5′-AACCCGCTGCTGATGA-3′	Sense	1093–1108	88	NM_173338	40	60
	5′-GCAAGTGGTAAGGCAGAA-3′	Anti-sense	1163–1180				

overnight at appropriate dilutions (see Table 1). Secondary antibodies from SuperPicture HRP Polymer Conjugate Kit for goat primary antibody (Invitrogen) for IHC or secondary antibodies appropriately conjugated with either FITC-488 or CY3-555 (Invitrogen) for IF microscopy were used. Images were captured using an Olympus BX61 fluorescence microscope with an Olympus DP71 (at 12·5 megapixel) digital camera and Olympus MicroSuite Five imaging software package to obtain the TIFF file format. All images were subsequently compiled and analyzed using Adobe Creative Suite CS3 software package, such as for image overlay. Each IHC and dual-labeled IF analysis experiment was repeated at least three times using different rat testis and/or Sertoli cell preparations. Thus, representative results from at least three independent experiments were shown herein.

Functional assessment of the Sertoli cell TJ permeability barrier

The Sertoli cell TJ permeability barrier was quantified by the ability of the cell epithelium to restrict the current flow (ohm) transmitted across the cell monolayer when two electrodes of a Millipore Millicell-ERS were placed in the corresponding apical and basal chamber of the bicameral unit (Millipore, Bedford, MA, USA), and a short (~2 seconds) 20 μAmp pulse of current was sent across the electrodes (i.e. the cell epithelium) as described earlier (Grima *et al*. 1998, Lui *et al*. 2001). In short, Sertoli cells cultured in F12/DMEM were plated on Matrigel-coated bicameral units (in triplicates) at $1{\cdot}2\times10^6$ cells/cm^2 at time 0, and TER was recorded daily, with fresh F12/DMEM replenished after the TER measurement. On day 3, when the TJ permeability barrier was established as manifested by a stable TER across the Sertoli cell epithelium, transfection was performed to silence either Oatp3 (*Slco1a5*) alone or in combination with three other drug influx pumps, namely OCTN2 (*Slc22a5*), TST-1 (*Slco6b1*) and TST-2 (*Slco6c1*) using the corresponding siRNA duplexes versus the non-targeting control siRNA duplexes to assess the effects of RNAi on the Sertoli cell TJ permeability barrier function.

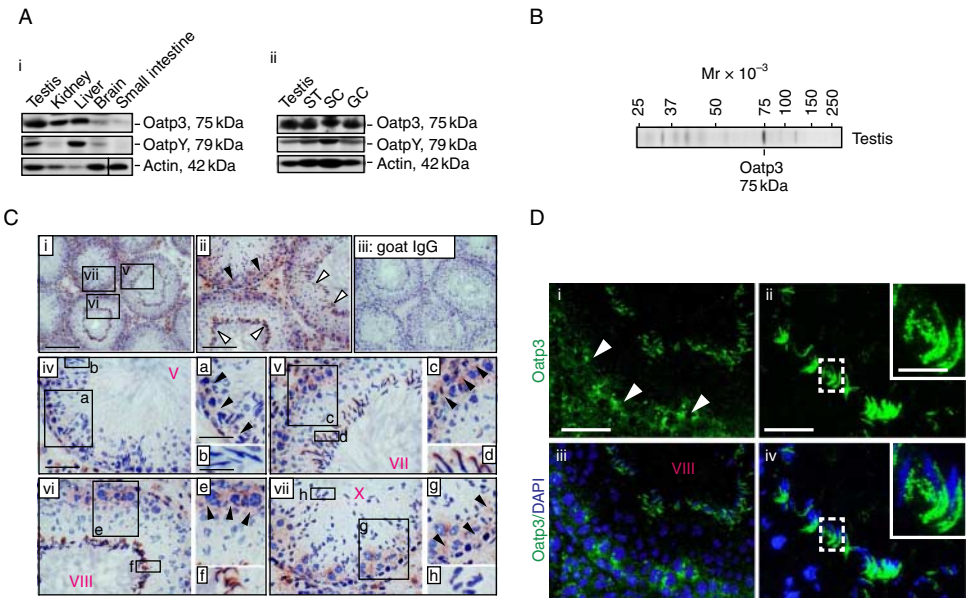

Figure 1 Cellular distribution of Oatp3 in the seminiferous epithelium of adult rat testes. (A) Immunoblot analysis using tissue lysates (~100 μg protein) of testes, kidney, liver, brain, small intestine, seminiferous tubules (ST) (these organs or tissues were all obtained from adult male rats), Sertoli cells (SC; from 20-day-old rats), and germ cells (GC; from adult rats) and a specific anti-Oatp3 or anti-OatpY antibody (see Table 1) (A i and ii). Actin served as a protein loading control. (B) An immunoblot illustrating the specificity of the anti-Oatp3 antibody with lysate from testes, which was used for immunohistochemistry (C) and immunofluorescence microscopy (D). (C) Localization of Oatp3 in the seminiferous epithelium by immunohistochemistry using frozen sections of testes and the anti-Oatp3 antibody (Table 1) (see i–ii, iv–vii, with iii as a negative control using normal goat IgG instead of the anti-Oatp3 antibody). Immunoreactive Oatp3 (reddish brown) was detected at the BTB (black arrowheads) in virtually all stages of the epithelial cycle but most prominently (and the highest expression) at stages VII–X. Intensive Oatp3 staining was also found at the apical ES (white arrowheads) in stage VII–VIII tubules, which became relatively weaker at other stages. In C, a–b, c–d, e–f, and g–h are magnified images of the corresponding boxed areas shown in iv, v, vi and vii. V, VII, VIII, X in 'red' refer to stages of tubules. Scale bar, 200 μm in C i, which applies to C iii; 100 μm in C ii; 50 μm in C iv, which applies to v, vi, and vii; 30 μm in a, which applies to c, e, and g; 20 μm in b, which applies to d, f, and h. (D) Immunofluorescence staining pattern of Oatp3 in rat testes. The stage-specific localization of Oatp3 in the testis shown in i–iv in D, such as at the BTB (white arrowheads in i) and the apical ES (see ii and iv) is consistent with findings in C. Insets in ii and iv are the magnified images of the corresponding boxed areas at the apical ES. iii–iv are the merged images of i–ii wherein cell nuclei were stained with DAPI. 50 μm in D i, which applies to iii; 20 μm in D ii, which applies to iv; 10 μm in inset in D ii, which applies to inset in D iv. Full colour version of this figure available via http://dx.doi.org/10.1530/JOE-10-0474.

RNA extraction and RT-PCR

As anti-OCTN2, anti-TST-1, and anti-TST-2 antibodies that could be used for immunoblot analysis were not available, we had used RT-PCR to assess the efficacy of their knockdown following RNAi. Total RNAs were extracted from Sertoli cells on day 3 after transfection with siRNA duplexes (see Table 2) using TRIzol reagent (Invitrogen). Contaminating genomic DNA in each RNA sample, if any, was digested with RNase-free DNase I (Invitrogen) prior to their use for reverse transcription into cDNAs using Moloney murine leukemia virus reverse transcriptase (M-MLV RT) reagent (Invitrogen). PCR was performed as described (Lui *et al.* 2003*a*, Su *et al.* 2009) using primer pairs specific to corresponding target genes (Table 3) and co-amplified with ribosomal S16, which served as an internal control for equal sample processing and RNA loading.

Quantitative real-time RT-PCR and data analysis

To further confirm the extent of gene silencing by RNAi as specific and/or working antibodies are not available for some influx pump transporters (e.g. *Slc22a5*, *Slco6b1*, and *Slco6c1*), quantitative real-time RT-PCR (qPCR) was used. qPCR was performed using an Applied Biosystems (Foster City, CA, USA) Prism 7700 Sequence Detection System with SYBR Green PCR Master Mix and primer pairs listed in Table 4. Primers for qPCR were designed using either the Oligonucleotide Properties Calculator at www.basic.northwestern.edu/biotools/oligocalc.html or the Primer Express (Version 2.0) from Applied Biosystems, Inc., and were compared with existing database at GenBank using the basic local alignment search tool (BLAST) to ensure specificity (Table 4). qPCR was performed at the Rockefeller University Genomics Resource Center as described earlier (Xia *et al.* 2007). Equal amount of total RNA was then reverse transcribed using M-MLV RT with 2 μg RNA in a 25 μl reaction. Both primers (5 pmol each) and various templates (including serially diluted control testis cDNA for generating the standard curve) and 1 μl reverse transcription product as described above were mixed with 2× SYBR Green PCR Master Mix in a 25 μl final reaction volume. The thermal cycler conditions were 10 min at 95 °C, followed by two-step (15 s at 95 °C and 1 min at 60 °C) PCR for 40 cycles, and a slow heating up to 95 °C for dissociation analysis at the end to ensure the purity of the PCR product. Amplification data analysis was performed using Applied Biosystems SDS 2.3 software as described in detail (Xia *et al.* 2007).

Statistical analysis

Statistical analyses were performed by two-way ANOVA with Tukey's honest significant test or Student's *t*-test using GB-STAT software (Version 7.0, Dynamic Microsystems, Silver Spring, MD, USA) to compare treatment and control groups as described (Yan *et al.* 2008*a*). Results of qPCR were analyzed by one-way ANOVA for multiple comparisons using the JMP IN statistical analysis software package (Version 4, SAS, Inc., Cary, NC, USA).

Results

*Stage-specific localization of Oatp3 (*Slco1a5*) in the seminiferous epithelium of adult rat testes*

Oatp3 displayed a broad tissue expression that was detected in testes, kidney, liver, brain and small intestine in adult male rats (~300 g b.w.) (Fig. 1Ai). In the testis, Oatp3 was found in the seminiferous tubules, Sertoli cells, and germ cells (Fig. 1Aii). The anti-Oatp3 antibody used for the various experiments reported in this study was selected based on the preliminary experiments when three anti-Oatp3 antibodies from different

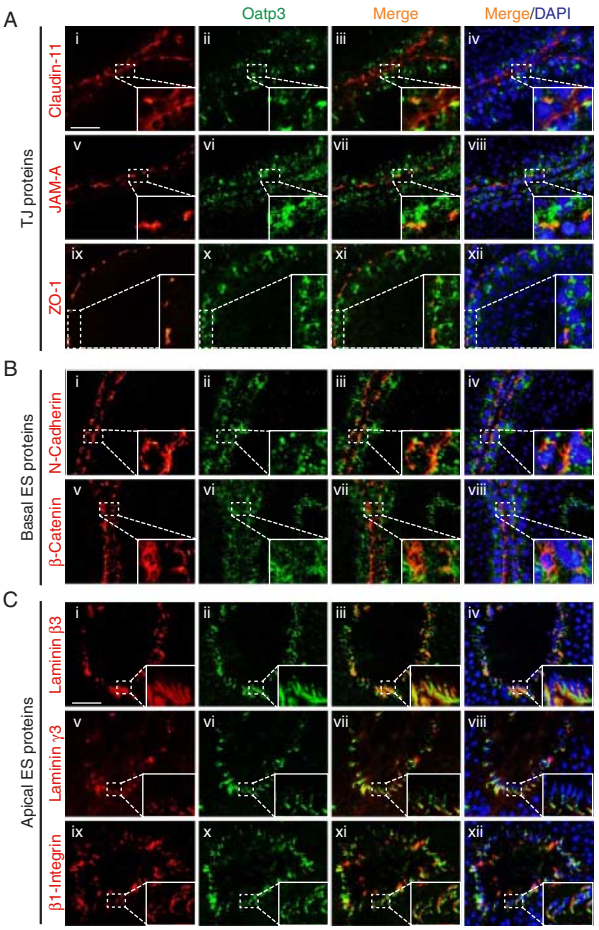

Figure 2 Dual-labeled immunofluorescence analysis on the co-localization of Oatp3 with putative BTB and apical ES proteins in the seminiferous epithelium. (A) Partial co-localization (see orange color) of Oatp3 with TJ proteins: claudin-11 (i–iv), JAM-A (v–viii), and ZO-1 (ix–xii) at the BTB. (B) Partial co-localization of Oatp3 with basal ES proteins: N-cadherin (i–iv) and β-catenin (v–viii) at the BTB. (C) Co-localization of Oatp3 with apical ES proteins: laminin β3 (i–iv), laminin γ3 (v–viii), and β1-integrin (ix–xii). Insets are magnified images of the corresponding boxed areas in the same micrographs. Scale bar: 50 μm in Ai, which applies to all images in B and C; 15 μm in inset in Ai, which applies to all insets in A, B, and C. Full colour version of this figure available via http://dx.doi.org/10.1530/JOE-10-0474.

vendors were compared, and its specificity was illustrated by immunoblot analysis (Fig. 1B and Table 1). Although this antibody yielded some faint staining for some unwanted proteins, it was the best antibody based on the initial pilot experiments (and at the selected dilution, the staining was shown to be specific based on pilot experiments using different dilutions) and appropriate dilutions were thus selected for different applications as noted in Table 1. Immunoreactive Oatp3 was detected near the basement membrane consistent with its localization at the BTB in almost all stages of the epithelial cycle, being highest at stages VII–X (Fig. 1C), at the time of BTB restructuring to facilitate the transit of preleptotene spermatocytes. Considerably weaker staining was detected at the BTB at stages III–V. Oatp3 staining was intense at the apical ES at stages VII–VIII, coinciding with spermiation that occurs at stage VIII of the epithelial cycle. Fluorescence microscopy also confirmed Oatp3 localization at the BTB and apical ES (Fig. 1D). Some Oatp3 staining was also found in the interstitial cells, associated with Leydig cells.

Co-localization of Oatp3 with junction proteins at the BTB and apical ES

Dual-labeled IF analysis was used to examine protein co-localization. At the BTB, Oatp3 displayed partial co-localization with TJ- (e.g. claudin-11, JAM-A, and ZO-1; Fig. 2A) and basal ES-proteins (e.g. N-cadherin and β-catenin; Fig. 2B). At the apical ES, Oatp3 almost superimposed with putative apical ES proteins: laminin β3, laminin γ3, and β1-integrin (Fig. 2C).

Changes in the expression and localization of Oatp3 during adjudin-induced germ cell loss in the testes

Adjudin ($C_{15}H_{12}Cl_2N_4O$, Mr 335·18), a potential male contraceptive, is known to induce germ cell loss from the seminiferous epithelium by perturbing, most notably, apical ES (Mruk *et al.* 2008). In adult rats treated with adjudin, the increase in Oatp3 was noted at 3 h after adjudin administration (Fig. 3Ai–ii). This increase maintained for ∼1 day but declined rapidly and was significantly lower by day 4, suggesting that testis 'shut-off' the influx pump to prevent entry of adjudin (note: adjudin is a toxicant for spermatogenesis) into the apical compartment by reducing the expression of Oatp3. As adjudin induced testis weight loss (Fig. 3Aiii) because of germ cell depletion from the seminiferous epithelium and the cellular composition in the samples being analyzed for Oatp3 and OatpY and shown in Fig. 3A:ii did not account for these changes, the data in Fig. 3A:ii were corrected for testis weight changes and shown in Fig. 3A:iv, illustrating a transient increase in Oatp3 expression indeed occurred and it was reduced by days 2–4 but not OatpY. Changes in the localization of Oatp3 in the seminiferous epithelium during adjudin-induced germ cell loss were also examined (Fig. 3B). Oatp3 was detected at both BTB and the apical ES in normal stage VIII tubules (Fig. 3Bi, a negative control shown in Fig. 3Bv) similar to findings shown in Fig. 1C. A stage V–VI tubule was found to have adjudin-induced misaligned spermatids 12 h after drug administration with intense Oatp3 staining at the apical ES (Fig. 3Bii), which was not seen in a normal stage V–VII tubule (see Fig. 1). When these spermatids are depleting from the epithelium, considerably more Oatp3 was found that surrounded these

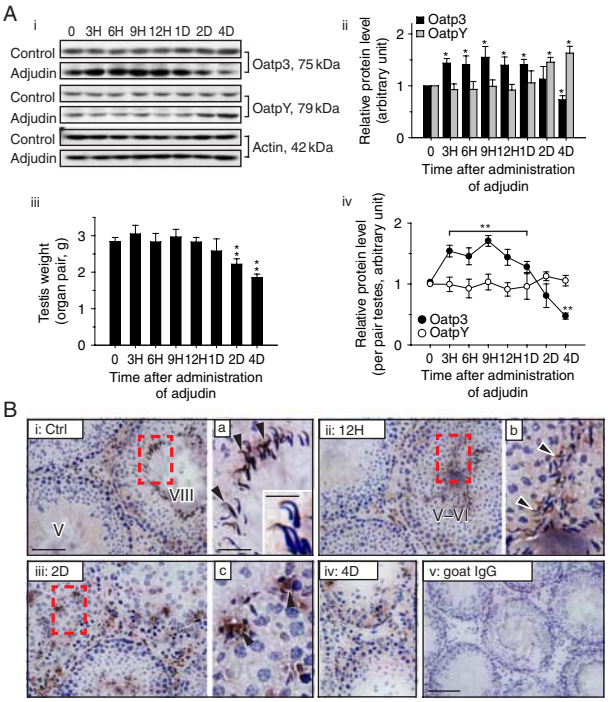

Figure 3 Changes in the steady-state levels and/or cellular distribution of Oatp3 versus OatpY during adjudin-induced anchoring junction restructuring in the seminiferous epithelium that leads to germ cell loss from the testis. (A) Representative immunoblotting results illustrating changes in steady-state levels of Oatp3 and OatpY in the testis after adjudin treatment (single dose at 50 mg/kg b.w., by gavage) administered to adult rats (∼300 g b.w.) at time 0 (A i). Composite immunoblot results (n=3–5 rats) such as those shown in i normalized against actin, wherein the elative protein level at time 0 in (A i) was arbitrarily set at 1, against which statistical analysis was performed (A ii). Bar graphs showing changes of testis weight during development and after adjudin treatment (A iii). Line graphs showing composite protein level changes of Oatp3 versus OatpY per pair testes (A iv). Each bar is the mean ± S.D. of n=3–5 rats. *P<0·05; **P<0·01 by ANOVA. (B) Frozen sections of testes from normal (B i) and adjudin-treated (B ii–iv) adult rats were immunostained with anti-Oatp3 antibody. Oatp3 staining was detected at the Sertoli–elongated spermatid interface (black arrowheads) at the apical ES in control (B i) and 12 H after (B ii) adjudin treatment and also at the Sertoli–round spermatid interface (black arrowheads) at the desmosome-like junction in 2 D (B iii) and 4 D (B iv) after adjudin treatment. (B v) Negative control in which normal goat IgG was used to substitute the anti-Oatp3 antibody. B a–c are the magnified images of the corresponding boxed areas in B i–iii. Inset in B a is a further enlarged area to illustrate the localization of Oatp3 at the apical ES. Scale bar: 100 μm in B i, which applies to ii–iv; 200 μm in B v; 50 μm in a, which applies to b, c; 15 μm in inset in a. Full colour version of this figure available via http://dx.doi.org/10.1530/JOE-10-0474.

cells, including the Sertoli cell-round spermatid interface (Fig. 3Biii–iv), seemingly suggesting that this influx pump might have allowed more adjudin to reach these misaligned spermatids to cause their defoliation.

Does Oatp3, an integrated component of adhesion protein complexes at the BTB, regulate drug entry to the testis?

Oatp3 was shown to structurally associate with components of adhesion protein complexes at the BTB including basal ES proteins N-cadherin, β-catenin, ZO-1, and actin, but not TJ-proteins occludin, FAK, and c-Src by Co-IP (Fig. 4A). This finding was further confirmed by dual-labeled IF analysis illustrating the co-localization of Oatp3 with ZO-1, N-cadherin, and β-catenin at the Sertoli–Sertoli cell interface (Fig. 4B). To further explore the role of Oatp3 in drug entry to the testis, Sertoli cells cultured for 3 days with an established TJ barrier was incubated with adjudin at 1 μg/ml for various time points (Fig. 4C). After adjudin treatment, the steady-state level of Oatp3 was upregulated by 1·5-fold from days 1–3 (Fig. 4C) and its staining intensity at Sertoli–Sertoli interface was also induced versus control (Fig. 4D). An increase in association between Oatp3 and ZO-1, β-catenin, or actin after adjudin treatment was also detected (Fig. 4E), suggesting that more

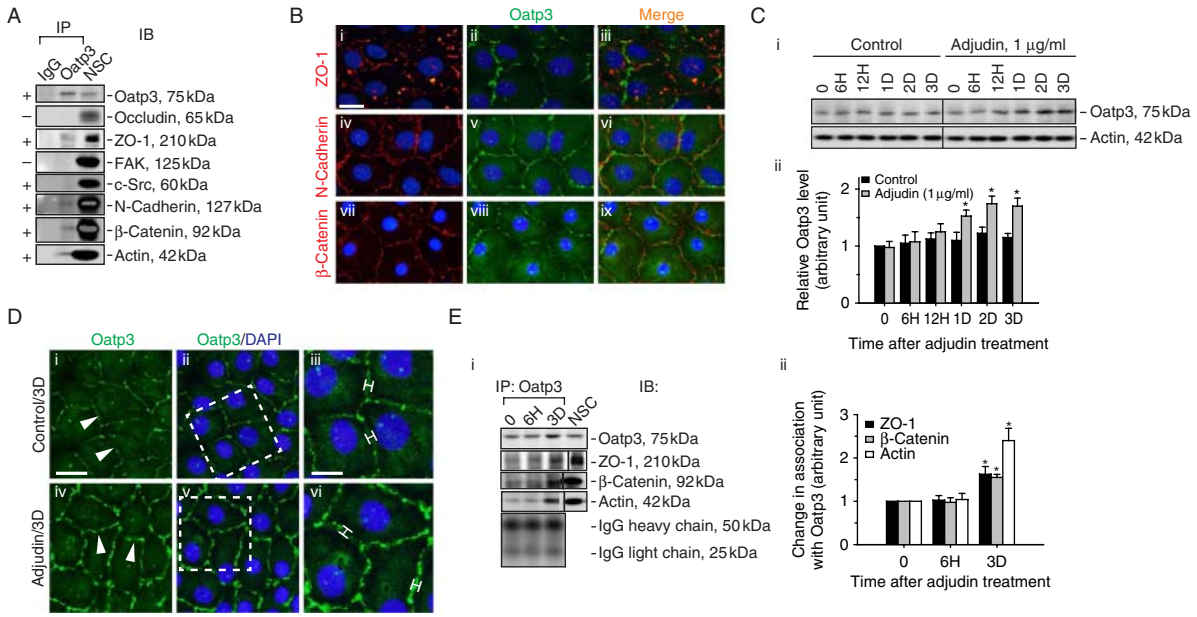

Figure 4 A study to examine the binding partners of Oatp3 and changes in protein–protein interactions at the BTB in Sertoli cell epithelium *in vitro* following treatment with adjudin. (A) Co-IP was performed using lysates (~300 μg protein) from Sertoli cells ($0{\cdot}5\times10^6$ cells/cm^2 cultured alone for 4 days on Matrigel-coated dishes, forming an intact cell epithelium and the presence of a functional TJ permeability barrier, see Fig. 5, with ultrastructures of TJ, basal ES, and desmosome-like junction when examined by electron microscopy (Siu *et al.* 2005) that mimicked the Sertoli cell BTB *in vivo*), Oatp3 was shown to structurally interact with ZO-1, N-cadherin, β-catenin, and actin (indicated by '+'), but not occludin, FAK, or c-Src (indicated by '−'). Sertoli cell lysates Co-IP with normal goat IgG (IgG) and Sertoli cell lysates alone without Co-IP (NSC) served as the corresponding negative and positive control. This experiment was repeated three times using different batches of Sertoli cell cultures that yielded similar results. (B) Dual-labeled immunofluorescence analysis illustrating co-localization of Oatp3 with ZO-1, N-cadherin, and β-catenin at the Sertoli–Sertoli cell interface. Scale bar: 15 μm in i, which applies to ii–ix. (C) Immunoblot (top panel) using Sertoli cell lysates wherein cells were treated with adjudin (1 μg/ml) on day 4 after an intact cell epithelium had been formed for specified time points to assess change in the steady-state level of Oatp3 (C i). Actin blot (lower panel) served as a loading control. These findings were summarized in a bar graph illustrating an upregulation of Sertoli cell Oatp3 expression induced by adjudin from day 1 through 3 post-treatment (C ii). Relative Oatp3 level at time 0 in control group was arbitrarily set as 1, against which statistical analysis was performed. Each bar is the mean ±S.D. of $n=4$ using different batches of Sertoli cells. *$P<0{\cdot}05$ by ANOVA. (D) Immunofluorescence microscopy (see i–vi) was used to verify data shown in (C) illustrating a brighter and broader staining pattern of Oatp3 (see bars in iii versus vi) at the Sertoli–Sertoli cell interface (white arrowheads in i and iv) by 3 days after adjudin treatment. iii and vi are enlarged images of the corresponding boxed areas in D ii and v. Nuclei were stained with DAPI. Scale bar: 15 μm in i, which applies to ii, iv, and v; 7 μm in iii, which applies to vi. (E) Co-IP to assess changes in association of Oatp3 with ZO-1, β-catenin, or actin following adjudin treatment using ~300 μg protein lysate per sample tube (E i). Normal Sertoli cell lysate without Co-IP was used as positive control (NSC). The bottom panel is the IgGH and IgGL chains, illustrating equal protein loading in this Co-IP experiment and that there was indeed an increase in association between ZO-1, β-catenin, and actin with Oatp3 during adjudin-induced anchoring junction restructuring in the epithelium. Densitometric analyses of blots such as those shown in (E i), illustrating an increase in association between these proteins (E ii). Relative association of the target protein with Oatp3 at time 0 was arbitrarily set as 1. Each bar is the mean±S.D. of $n=3$. *$P<0{\cdot}05$ by ANOVA. Full colour version of this figure available via http://dx.doi.org/10.1530/JOE-10-0474.

Oatp3 was 'recruited' to the BTB site to facilitate drug entry to the seminiferous epithelium. We next investigated whether the effects of influx pump to regulate drug entry would impede the Sertoli cell TJ permeability barrier function.

The influx pump function of Oatp3 appears to operate independent of the TJ permeability barrier function

As Oatp3 is an integrated component of the N-cadherin-based adhesion protein complex at the BTB, we sought to examine whether Oatp3 knockdown would impede the Sertoli cell TJ barrier function (Fig. 5A–G). On day 3 after Sertoli cells established a function TJ barrier (Fig. 5G), cells were transfected with the specific *Oatp3* siRNA duplexes versus the non-targeting control siRNA duplexes. While a ~60% knockdown of Oatp3 was noted (Fig. 5A and B) with the concomitant disappearance of Oatp3 from the cell–cell interface (Fig. 5C) without off-target effects as far as we examined (Fig. 5A and E; for instance, P-glycoprotein and mrp1, both are efflux pumps, was not affected, similar to other BTB proteins), the Sertoli cell TJ barrier was not perturbed (Fig. 5D, F and G).

Quadruple knockdown of MIDTs by RNAi does not affect the Sertoli cell TJ permeability function

To further validate the concept that the drug transport function at the BTB mediated by influx pumps may be segregated from the TJ barrier function even though drug transporters physically interact with adhesion protein complexes at the BTB, we sought to perform quadruple knockdown of several influx drug pumps in Sertoli cell epithelium and to assess the TJ barrier integrity. Based on the two earlier studies (Augustine *et al.* 2005, Su *et al.* 2009), besides Oatp3 (*Slco1a5*), *Slc22a5*, *Slco6b1*, and *Slco6c1* are the major influx drug pumps in Sertoli cells, thus these four drug transporters (MIDTs) were selected for the subsequent experiments. When these four influx pumps were

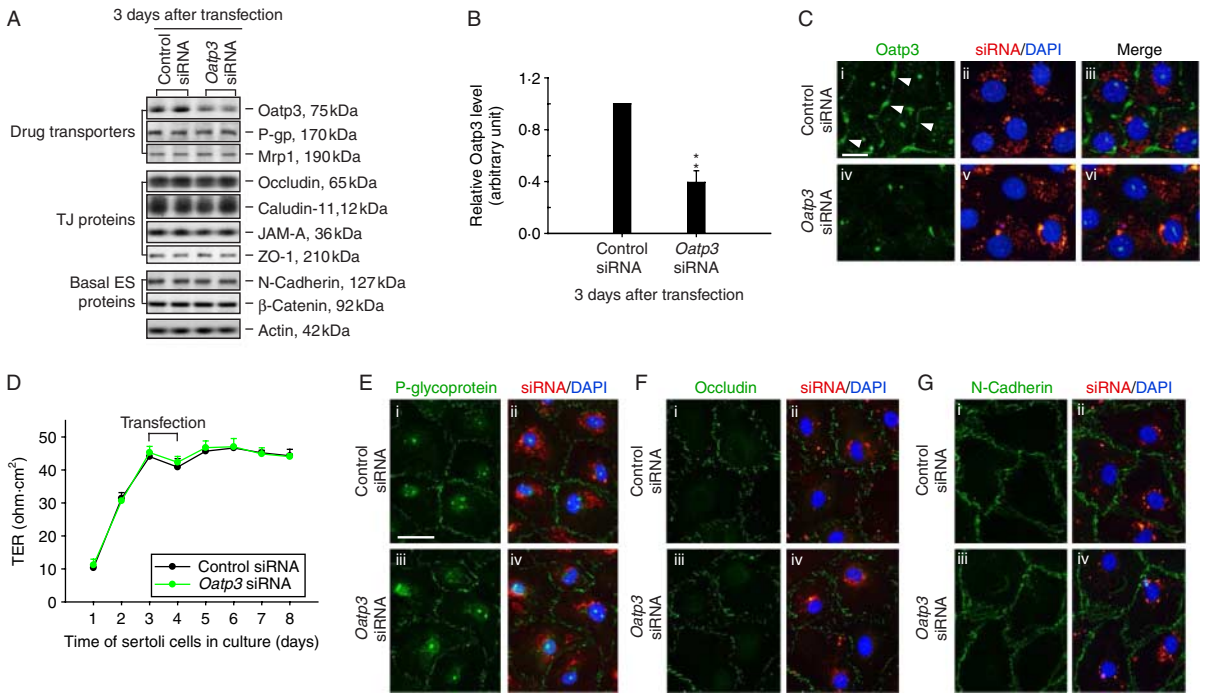

Figure 5 A study to assess any changes on the Sertoli cell BTB function and protein distribution following the knockdown of Oatp3 by RNAi. (A) Sertoli cells cultured at $0{\cdot}5\times10^6$ cells/cm^2 on Matrigel-coated dishes on day 3 with an established intact cell epithelium were transfected with 100 nM *Oatp3*-specific siRNA duplexes versus non-targeting control duplexes, cells were harvested 3 days thereafter. (B) Although a ≈60% decline in the steady-state protein level of Oatp3 was noted, no changes in two major efflux drug transporters, P-glycoprotein (P-gp) and Mrp1, or other TJ and basal ES junction proteins were detected illustrating no off-target effects (A). $^{**}P<0{\cdot}01$ by Student's *t*-test. (C) Sertoli cells cultured at $0{\cdot}05\times10^6$ cells/cm^2 for 3 days were transfected with CY3-labeled *Oatp3*-specific siRNA duplexes (red) and non-targeting control duplexes (red) for 24 h and were staining with anti-Oatp3 antibody (green). Much of the immunoreactive Oatp3 at the Sertoli–Sertoli cell interface (arrowheads) was diminished considerably after RNAi when compared with controls (iv–vi versus i–iii). (D) The Sertoli cell TJ permeability barrier function was also monitored by quantifying transepithelial electrical resistance (TER) across the cell epithelium after Oatp3 RNAi versus controls, illustrating no effect of Oatp3 knockdown on Sertoli cell TJ barrier function. (E–G) Oatp3 knockdown did not affect the distribution of P-glycoprotein (E iii–vi versus i–ii), occludin (F iii–vi versus i–ii) or N-cadherin (G iii–vi versus i–ii) at the Sertoli–Sertoli cell interface. Scale bar, 15 μm in C i, which applies to ii–vi; 30 μm in E i, which applies to ii–iv and also i–iv in both F and G. Full colour version of this figure available via http://dx.doi.org/10.1530/JOE-10-0474.

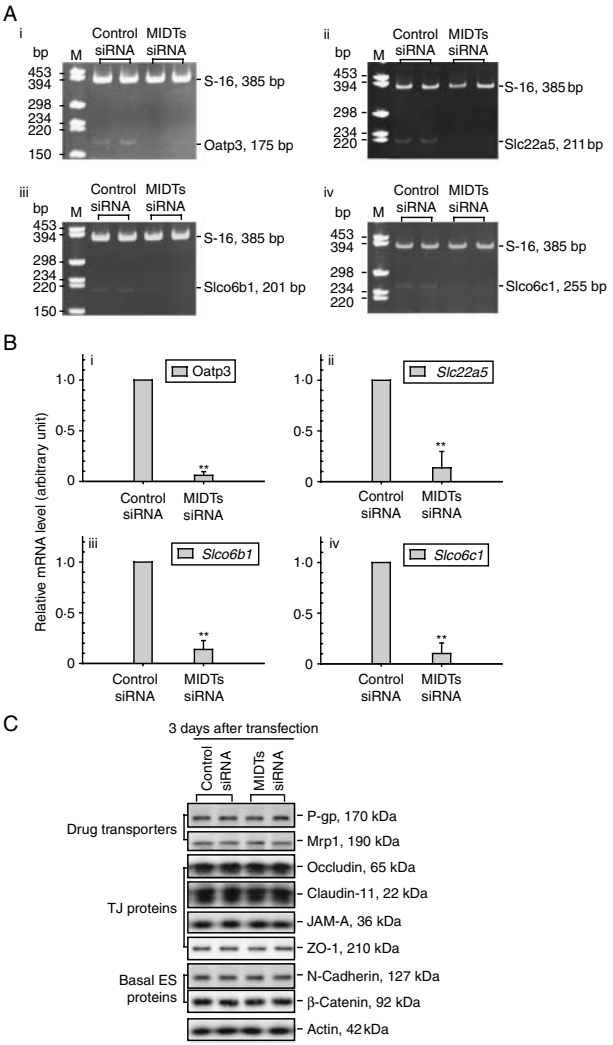

Figure 6 A study to assess the efficacy of simultaneous knockdown of multiple influx drug transporters (MIDTs): Oatp3 (*Slco1a5*), *Slc22a5*, *Slco6b1*, and *Slco6c1* by RNAi without off-target effects. (A) Sertoli cells isolated from 20-day-old rat testes were plated at time 0 and cultured at $0{\cdot}5\times10^6$ cells/cm^2 to allow the establishment of a functional TJ barrier. On day 3, these cultures were transfected with 200 nM MIDT (50 nM each)-specific siRNA duplexes versus non-targeting control siRNA duplexes for 24 h, and cells were terminated for RNA extraction 3 days thereafter to assess silencing efficacy. RT-PCR illustrated that the quadruple knockdown of Oatp3 (i), *Slc22a5* (ii), *Slco6b1* (iii), and *Slco6c1* (iv) reduced the corresponding steady-state mRNA level by ~70–80% for each target gene with S-16 served as an internal control. (B) The findings in (A) were validated by qPCR shown in (i)–(iv) for the corresponding target influx pump transporters with an ~70–80% knockdown. $^{**}P<0{\cdot}01$ by ANOVA. (C) Immunoblot analysis showed that there was no off-target effect following the knockdown of MIDTs as multiple proteins including P-glycoprotein (P-gp, an efflux pump) and multidrug resistance-associated protein 1 (Mrp1) were not affected, illustrating that the silencing is specific to the corresponding target drug transporter.

knockeddown by RNAi using corresponding siRNA duplexes versus control duplexes with ~70–80% efficacy (up to >95% efficacy in some cases) when verified by RT-PCR and qPCR (Fig. 6A and B), no off-target effects were detected (Fig. 6C), illustrating the specificity of the RNAi experiments. Consistent with results shown in Fig. 5, the quadruple knockdown of MIDTs did not perturb the Sertoli cell TJ barrier function (Fig. 7A) nor the distribution of occludin or N-cadherin at the Sertoli–Sertoli cell interface (Fig. 7B), confirming that the TJ barrier integrity was not compromised.

A knockdown of Oatp3 or MIDTs by RNAi impedes the transit of [^{3}H]adjudin at the BTB in Sertoli cell epithelium

The entry of drugs, such as adjudin, into the microenvironment, namely the apical compartment, behind the BTB in the testis remains unknown (Mruk & Cheng 2008) when receptors are not present in Sertoli cells. For instance, adjudin has exceedingly poor bioavailability (Cheng *et al.* 2005), possibly due to the lack of a specific a receptor. In this study, we tested the hypothesis that drug entry into the testis is mediated by drug transporters by RNAi. On day 3, Sertoli cells having an established TJ barrier were transfected with corresponding siRNA duplexes to knockdown either Oatp3 alone or MIDTs, and 3 days thereafter when these genes were silenced (see Fig. 6A–C), [^{3}H]adjudin was added to the basal compartment of the bicameral units at time 0. At specified time points as shown in Fig. 7C, an aliquot of 50 μl medium was withdrawn from the apical and basal compartment for radioactivity determination to quantify the movement of [^{3}H]adjudin across the Sertoli cell BTB when the TJ barrier was not compromised (Fig. 7A and B, Fig. 5D). A knockdown of Oatp3 alone impeded the transport of [^{3}H]adjudin across the Sertoli cell TJ barrier, but the quadruple knockdown of MIDTs impeded [^{3}H]adjudin considerably more effectively than Oatp3 knockdown alone (Fig. 7C). These findings illustrate that drug entry in the testis is mediated by influx drug pumps. Although Oatp3 is an integrated component of protein complexes that confer TJ barrier function at the BTB, drug entry into the epithelium behind the BTB is not mediated by a 'disruption' of the TJ barrier. Instead, it is mediated by a drug transport mechanism, involving at least influx pumps, independent of the TJ permeability barrier function.

Discussion

Does Oatp3, an influx pump and an integrated component of the N-cadherin-based adhesion protein complex, regulate the Sertoli cell TJ permeability barrier function?

ATP-binding cassette transporters, such as P-glycoprotein (a multidrug resistance protein) and breast cancer resistance protein that are expressed by Sertoli cells, peritubular myoid

cells, and germ cells (most notably late spermatids) in the testis (for a review, see Setchell (2008)), are efflux pumps that actively transport drugs 'out' of epithelial or endothelial cells, or 'prevent' drugs from entering cells, utilizing a primary active transport mechanism utilizing ATP (Dallas *et al.* 2006, Miller *et al.* 2008, Shen & Zhang 2010). Unlike these efflux pump transporters, influx pumps, such as SLC transporters, including Oatp3, OCTN2 (*Slc22a5*), TST-1 (*Slco6b1*), and TST-2 (*Slco6c1*) that were examined in this report, that transport drugs 'into' epithelial or endothelial cells utilize one of the two non-ATP-dependent mechanisms (El-Sheikh *et al.* 2008, Kis *et al.* 2010, Ueno *et al.* 2010). First, the energy that pumps drugs or small molecules into cells via an influx pump derives from a gradient that is created by a primary active transport system such as the electrochemical potential difference created by pumping ions (e.g. Na^+ and K^+). Secondly, drugs, ionic compounds, or heavy metals enter cells via the 'pores' in SLC transporters. Since Oatp3 is an integrated component of the N-cadherin-based cell adhesion protein complex at the BTB that structurally interacts with N-cadherin, β-catenin, and ZO-1, but not occludin or FAK (note: FAK forms a regulatory protein complex with occludin at the BTB (Siu *et al.* 2009*b*)) as reported in this study, we speculated that these influx pumps might mediate their effects to transport drugs across the Sertoli cell BTB via changes in the TJ permeability barrier. In fact, the protein–protein

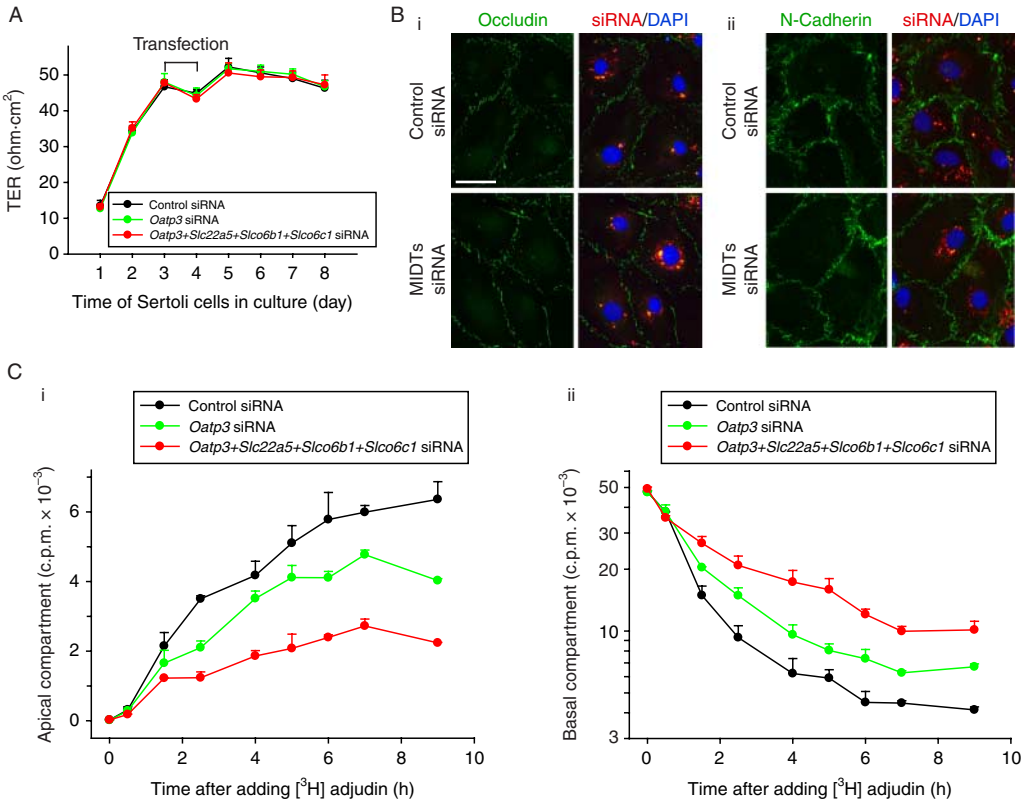

Figure 7 A study to assess the effects of simultaneous knockdown of multiple influx drug transporters (MIDTs): Oatp3 (*Slco1a5*), *Slc22a5*, *Slco6b1*, and *Slco6c1* by RNAi on the Sertoli cell TJ permeability function as well as the ability of drug transport across the BTB assessed by [^{3}H]adjudin entry from the basal to the apical compartment. (A) The silencing of Oatp3 alone (50 nM *Oatp3* siRNA +150 nM control siRNA) or all four drug influx pumps (50 nM for each drug transporter to a total of 200 nM siRNA duplexes) versus non-targeting control siRNA duplexes (200 nM) failed to perturb the Sertoli cell TJ barrier function when TER across the cell epithelium was monitored. (B) Dual-labeled immunofluorescence analysis illustrated that there were no changes in the distribution of occludin (i) or N-cadherin (ii) at the Sertoli–Sertoli cell interface after MIDTs knockdown. Scale bar, 30 μm in D i, which applies to remaining micrographs in both D i and ii. (C) A study to assess the effects of Oatp3 knockdown or quadruple MIDTs knockdown by RNAi on the transport of [^{3}H]adjudin cross the Sertoli cell epithelium. Sertoli cells were cultured alone on Matrigel-coated bicameral units at $1{\cdot}2\times10^6$ cells/cm^2 for 3 days, forming an intact cell epithelium, and thereafter, cells were transfected with non-targeting control, Oatp3-specific, or MIDTs siRNA duplexes for 24 h. After 2 days (i.e. 3 days after initial transfection) when targeted drug transporters: Oatp3 alone or Oatp3, *Slc22a5*, *Slco6b1*, and *Slco6c1* were being knockeddown (see C: i), [^{3}H]adjudin (~$0{\cdot}6\times10^6$ c.p.m.) was added to the basal compartment of the bicameral units and this time was designated time 0. At selected time points from 0 to 9 h, 50 μl F12/DMEM was withdrawn from apical (C: i, linear scale) or basal (C: ii, common log scale) compartments (note: each compartment contained 500 μl F12/DMEM) of the bicameral units for radioactivity determination in the presence of scintillation fluid using a β-counter. Each data point contains triplicate determinations from both control and experiment groups, and this experiment was repeated three times using different batches of Sertoli cell cultures. Full colour version of this figure available via http://dx.doi.org/10.1530/JOE-10-0474.

interaction between Oatp3 and ZO-1 or β-catenin was significantly induced following adjudin treatment, plausibly being used to reinforce the BTB integrity to prevent the entry of adjudin into the apical compartment of the epithelium where post-meiotic spermatid development takes place because adjudin is 'viewed' as a toxicant in relation to spermatogenesis. Furthermore, a recent study has shown that P-glycoprotein is also an integrated component of the occludin-, claudin-11-, and JAM A-based adhesion protein complexes at the BTB (Su *et al.* 2009). Collectively, these findings thus support the postulate that the presence of drug transporters at the BTB may facilitate or be involved in the maintenance of the Sertoli cell TJ permeability barrier. Surprisingly, a knockdown of Oatp3 alone or a combination of Oatp3 and three other SLC transporters, namely OCTN2 (*Slc22a5*), TST-1 (*Slco6b1*), and TST-2 (*Slco6c1*) did not perturb the Sertoli cell TJ barrier nor protein distribution at the Sertoli–Sertoli cell interface (e.g. occludin and N-cadherin) even though the amount of immunoreactive Oatp3 at the cell–cell interface significantly subsided as a result of the knockdown by RNAi. These findings thus demonstrate unequivocally that even though Oatp3, a SLC transporter and an influx pump, is an integrated component of the adhesion complexes at the BTB, its knockdown does not impede the Sertoli cell TJ barrier function, making it unlikely that drugs can traverse the BTB via an alteration in the TJ barrier function induced by changes in protein–protein interactions between influx pumps and cell adhesion proteins at the site. In this context, it is noted that the Sertoli cell *in vitro* system to study BTB function is widely used in the field (Janecki *et al.* 1991*b*, 1992) and numerous findings obtained based on this *in vitro* system (Lui *et al.* 2003*a*, Siu *et al.* 2003) have been reproduced in studies *in vivo* using a BTB integrity assay (Lui *et al.* 2003*b*, Li *et al.* 2006, Xia *et al.* 2009). In short, this is a reliable system to study Sertoli cell BTB dynamics.

Transport of drug (e.g. adjudin) across the BTB is mediated almost exclusively by influx pumps instead of paracellular transport through the TJ barrier

In an earlier study examining the distribution and organ uptake of [^{3}H]adjudin in the testis versus other organs (such as liver, kidney, brain, and small intestine) to assess its bioavailability, it was shown that this drug distributed almost evenly amongst all organs examined with $<0{\cdot}05\%$ of the total administered reaching the testis and $>95\%$ being cleared from host animals within 24–48 h (Cheng *et al.* 2005). Even though the BTB poses an excellent barrier to adjudin, this compound (at 50 mg/kg b.w., by gavage) limits its effects almost exclusively in the testis by disrupting the testis-specific anchoring junction namely apical ES at the Sertoli–spermatid interface because at up to 2000 m/kg b.w. in rats or 1000 mg/kg b.w. in mice (Ames test), no damage was seen in other organs when performed by licensed toxicologists and results from serum microchemistry also illustrated no associated liver or kidney damage was detected (Mruk *et al.* 2006, Mruk & Cheng 2008). Because of the knockdown of either Oatp3 alone or in combination with three other Sertoli cell major SLC influx transporters failed to alter the TJ permeability barrier as reported in this study, these findings suggest that drug transport across the BTB may not be mediated via a transiently 'disrupted' BTB. Instead, the findings reported in this study illustrate that the entry of [^{3}H]adjudin across the Sertoli cell BTB into the apical compartment of the bicameral units was significantly impeded when the expression of Oatp3 was knockeddown by RNAi using specific *Oatp3* siRNA duplexes, and the quadruple knockdown of four SLC transporters further impeded the transport of [^{3}H]adjudin across the Sertoli cell BTB. Thus, drug entry at the BTB is likely mediated via the 'pores' located in the influx pumps instead of a transiently 'disrupted' Sertoli cell TJ barrier. This information is extremely helpful in male contraceptive development, in particular, using compounds (e.g. adjudin) that likely exert their effects in the apical compartment of the seminiferous epithelium behind the BTB. In this context, it is of interest to note that $\sim$10% of [^{3}H]adjudin added onto the basal compartment of the bicameral unit could reach the apical compartment. However, earlier studies to assess the bioavailability of [^{3}H]adjudin by administering this compound to adult rats orally and to assess its recovery in the testis illustrates that fewer than $\sim$1% could reach the seminiferous epithelium (Cheng *et al.* 2005), and this extremely low bioavailability is consistent with studies of pharmacokinetics to assess its tissue distribution in both rats (Mruk *et al.* 2006) and rabbits (Hu *et al.* 2009). This is likely due to the lack of myoid cell layer in the *in vitro* system because the myoid cell layer surrounding the seminiferous tubule is known to significantly contribute to the BTB function in rodents (Dym & Fawcett 1970, Fawcett *et al.* 1970), even though its role in primates (Dym 1973) and perhaps humans is considerably diminished. In short, these findings demonstrate that the entry of adjudin into the apical compartment of the seminiferous epithelium is mediated almost exclusively by drug transporters instead of via paracellular diffusion at the TJ barrier. Thus, these findings require additional studies to examine whether the transport of other drugs and/or chemicals across the BTB is similarly regulated. Additionally, it remains to be determined if a knockdown of efflux pumps (e.g. P-glycoprotein) would impede the Sertoli TJ permeability barrier function.

Concluding remarks

It must be noted that the above findings regarding the role of efflux pumps in mediating drug transport across the BTB is based on the use of an *in vitro* model of Sertoli cell BTB. Yet, it is also noted that many of the earlier findings using this *in vitro* model to study BTB regulation, such as the regulation of Sertoli cell TJ permeability barrier function *in vitro* by TGF-β3 (Lui *et al.* 2001) is mediated via the p38 MAPK signaling

pathway downstream (Lui *et al.* 2003*a*), have subsequently been confirmed and validated in studies *in vivo* (Lui *et al.* 2003*b*, Wong *et al.* 2004). This is not entirely unexpected because multiple laboratories have been using this *in vitro* primary Sertoli cell culture system to investigate the biology and regulation of BTB dynamics including our laboratory (Byers *et al.* 1986, Grima *et al.* 1992, Janecki *et al.* 1992, Okanlawon & Dym 1996, Chung & Cheng 2001, Li *et al.* 2001*b*), and many of these findings were subsequently confirmed in studies *in vivo* (Hew *et al.* 1993, Lui *et al.* 2003*b*, Wong *et al.* 2005). Nonetheless, these findings reported in this study require additional *in vivo* studies for their validation.

Declaration of interest

The authors declare that there is no conflict of interest that could be perceived as prejudicing the impartiality of the research reported.

Funding

This research was supported by grants from the National Institutes of Health (NICHD, R01 HD056034 and R01 HD056034-02-S1 to C Y C; U54 HD029990 Project 5 to C Y C; R03 HD 061401 to DDM); and Research Grant Councils and Committee for Research and Conference Grants (CRGG) of the University of Hong Kong to WML.

Acknowledgements

We thank Dr Elissa W P Wong for her helpful suggestions in performing the real-time quantitative PCR experiments and her help in analyzing the qPCR data.

References

Abe T, Kakyo M, Sakagami H, Tokui T, Nishio T, Tanemoto M, Nomura H, Hebert SC, Matsuno S, Kondo H *et al.* 1998 Molecular characterization and tissue distribution of a new organic anion transporter subtype (oatp3) that transports thyroid hormones and taurocholate and comparison with oatp2. *Journal of Biological Chemistry* **273** 22395–22401. (doi:10.1074/jbc.273.35.22395)

Augustine LM, Markelewicz RJJ, Boekelheide K & Cherrington NJ 2005 Xenobiotic and endobiotic transporter mRNA expression in the blood–testis barrier. *Drug Metabolism and Disposition* **33** 182–189. (doi:10.1124/dmd.104.001024)

Byers S, Hadley M, Djakiew D & Dym M 1986 Growth and characterization of epididymal epithelial cells and Sertoli cells in dual environment culture chambers. *Journal of Andrology* **7** 59–68.

Cattori V, van Montfoort JE, Stieger B, Landmann L, Meijer DKF, Winterhalter KH, Meier PJ & Hagenbuch B 2001 Localization of organic anion transporting polypeptide 4 (Oatp4) in rat liver and comparison of its substrate specificity with Oatp1, Oatp2 and Oatp3. *Pflügers Archiv: European Journal of Physiology* **443** 188–195. (doi:10.1007/s004240100697)

Cheng CY & Mruk DD 2002 Cell junction dynamics in the testis: Sertoli–germ cell interactions and male contraceptive development. *Physiological Reviews* **82** 825–874. (doi:10.1152/physrev.00009.2002)

Cheng CY & Mruk DD 2010 A local autocrine axis in the testes that regulates spermatogenesis. *Nature Reviews. Endocrinology* **6** 380–395. (doi:10.1038/nrendo.2010.71)

Cheng CY, Mather JP, Byer AL & Bardin CW 1986 Identification of hormonally responsive proteins in primary Sertoli cell culture medium by anion-exchange high performance liquid chromatography. *Endocrinology* **118** 480–488. (doi:10.1210/endo-118-2-480)

Cheng CY, Silvestrini B, Grima J, Mo MY, Zhu LJ, Johansson E, Saso L, Leone MG, Palmery M & Mruk DD 2001 Two new male contraceptives exert their effects by depleting germ cells prematurely from the testis. *Biology of Reproduction* **65** 449–461. (doi:10.1095/biolreprod65.2.449)

Cheng CY, Mruk DD, Silvestrini B, Bonanomi M, Wong CH, Siu MKY, Lee NPY & Mo MY 2005 AF-2364 [1-(2,4-dichlorobenzyl)-*1H*-indazole-3-carbohydrazide] is a potential male contraceptive: a review of recent data. *Contraception* **72** 251–261. (doi:10.1016/j.contraception.2005.03.008)

Cheng CY, Wong EWP, Lie PPY, Li MWM, Su L, Siu ER, Yan HHN, Mannu J, Mathur PP, Bonanomi M *et al.* 2011 Environmental toxicants and male reproductive function. *Spermatogenesis* **1** 2–13. (doi:10.4161/spmg.1.1.13971)

Chung NPY & Cheng CY 2001 Is cadmium chloride-induced inter-Sertoli tight junction permeability barrier disruption a suitable *in vitro* model to study the events of junction disassembly during spermatogenesis in the rat testis? *Endocrinology* **142** 1878–1888. (doi:10.1210/en.142.5.1878)

Collarini EJ, Kuhn R, Marshall CJ, Monuki ES, Lemke G & Richardson WD 1992 Down-regulation of the POU transcription factor SCIP is an early event in oligodendrocyte differentiation *in vitro*. *Development* **116** 193–200.

Dallas S, Miller DS & Bendayan R 2006 Multidrug resistance-associated proteins: expression and function in the central nervous system. *Pharmacological Reviews* **58** 140–161. (doi:10.1124/pr.58.2.3)

Dym M 1973 The fine structure of the monkey (*Macaca*) Sertoli cell and its role in maintaining the blood–testis barrier. *Anatomical Record* **175** 639–656. (doi:10.1002/ar.1091750402)

Dym M & Fawcett DW 1970 The blood–testis barrier in the rat and the physiological compartmentation of the seminiferous epithelium. *Biology of Reproduction* **3** 308–326.

El-Sheikh AA, Masereeuw R & Russel FG 2008 Mechanisms of renal anionic drug transport. *European Journal of Pharmacology* **585** 245–255. (doi:10.1016/j.ejphar.2008.02.085)

Fawcett DW, Leak LV & Heidger PM 1970 Electron microscopic observations on the structural components of the blood–testis barrier. *Journal of Reproduction and Fertility* **10** (Supplement) 105–122.

Grima J, Pineau C, Bardin CW & Cheng CY 1992 Rat Sertoli cell clusterin, α_2-macroglobulin, and testins: biosynthesis and differential regulation by germ cells. *Molecular and Cellular Endocrinology* **89** 127–140. (doi:10.1016/0303-7207(92)90219-V)

Grima J, Wong CC, Zhu LJ, Zong SD & Cheng CY 1998 Testin secreted by Sertoli cells is associated with the cell surface, and its expression correlates with the disruption of Sertoli–germ cell junctions but not the inter-Sertoli tight junction. *Journal of Biological Chemistry* **273** 21040–21053. (doi:10.1074/jbc.273.33.21040)

Hew KW, Heath GL, Jiwa AH & Welsh MJ 1993 Cadmium *in vivo* causes disruption of tight junction-associated microfilaments in rat Sertoli cells. *Biology of Reproduction* **49** 840–849. (doi:10.1095/biolreprod49.4.840)

Hu GX, Hu LF, Yang DZ, Li JW, Chen GR, Chen BB, Mruk DD, Bonanomi M, Silvestrini B, Cheng CY *et al.* 2009 Adjudin targeting rabbit germ cell adhesion as a male contraceptive: a pharmacokinetics study. *Journal of Andrology* **30** 87–93. (doi:10.2164/jandrol.108.004994)

Janecki A & Steinberger A 1986 Polarized Sertoli cell functions in a new two-compartment culture system. *Journal of Andrology* **7** 69–71.

Janecki A, Jakubowiak A & Steinberger A 1991*a* Effects of cyclic AMP and phorbol ester on transepithelial electrical resistance of Sertoli cell monolayers in two-compartment culture. *Molecular and Cellular Endocrinology* **82** 61–69. (doi:10.1016/0303-7207(91)90009-H)

Janecki A, Jakubowiak A & Steinberger A 1991*b* Regulation of transepithelial electrical resistance in two-compartment Sertoli cell cultures: *in vitro* model of the blood–testis barrier. *Endocrinology* **129** 1489–1496. (doi:10.1210/endo-129-3-1489)

Janecki A, Jakubowiak A & Steinberger A 1992 Effect of cadmium chloride on transepithelial electrical resistance of Sertoli cell monolayers in two-

compartment cultures – a new model for toxicological investigations of the "blood–testis" barrier *in vitro*. *Toxicology and Applied Pharmacology* **112** 51–57. (doi:10.1016/0041-008X(92)90278-Z)

Kis O, Robillard K, Chan GN & Bendayan R 2010 The complexities of antiretroviral drug–drug interactions: role of ABC and SLC transporters. *Trends in Pharmacological Sciences* **31** 22–35. (doi:10.1016/j.tips.2009.10.001)

Klaassen CD & Aleksunes LM 2010 Xenobiotic, bile acid, and cholesterol transporters: function and regulation. *Pharmacological Reviews* **62** 1–96. (doi:10.1124/pr.109.002014)

Li JCH, Lee WM, Mruk DD & Cheng CY 2001*a* Regulation of Sertoli cell myotubularin (rMTM) expression by germ cells *in vitro*. *Journal of Andrology* **22** 266–277.

Li JCH, Mruk DD & Cheng CY 2001*b* The inter-Sertoli tight junction permeability barrier is regulated by the inter-play of protein phosphatases and kinases: an *in vitro* study. *Journal of Andrology* **22** 847–856.

Li MWM, Xia W, Mruk DD, Wang CQF, Yan HHY, Siu MKY, Lui WY, Lee WM & Cheng CY 2006 TNFα reversibly disrupts the blood–testis barrier and impairs Sertoli–germ cell adhesion in the seminiferous epithelium of adult rat testes. *Journal of Endocrinology* **190** 313–329. (doi:10.1677/joe.1.06781)

Li MWM, Mruk DD, Lee WM & Cheng CY 2009 Connexin 43 and plakophilin-2 as a protein complex that regulates blood–testis barrier dynamics. *PNAS* **106** 10213–10218. (doi:10.1073/pnas.0901700106)

Lie PPY, Cheng CY & Mruk DD 2010 Crosstalk between desmoglein-2/desmocollin-2/Src kinase and coxsackie and adenovirus receptor/ZO-1 protein complexes, regulates blood–testis barrier dynamics. *International Journal of Biochemistry and Cell Biology* **42** 975–986. (doi:10.1016/j.biocel.2010.02.010)

Lui WY, Lee WM & Cheng CY 2001 Transforming growth factor-β3 perturbs the inter-Sertoli tight junction permeability barrier *in vitro* possibly mediated via its effects on occludin, zonula occludens-1, and claudin-11. *Endocrinology* **142** 1865–1877. (doi:10.1210/en.142.5.1865)

Lui WY, Lee WM & Cheng CY 2003*a* Transforming growth factor-β3 regulates the dynamics of Sertoli cell tight junctions via the p38 mitogen-activated protein kinase pathway. *Biology of Reproduction* **68** 1597–1612. (doi:10.1095/biolreprod.102.011387)

Lui WY, Wong CH, Mruk DD & Cheng CY 2003*b* TGF-β3 regulates the blood–testis barrier dynamics via the p38 mitogen activated protein (MAP) kinase pathway: an *in vivo* study. *Endocrinology* **144** 1139–1142. (doi:10.1210/en.2002-0211)

Meier PJ & Stieger B 2002 Bile salt transporters. *Annual Review of Physiology* **64** 635–661. (doi:10.1146/annurev.physiol.64.082201.100300)

Meinhardt A & Hedger MP 2010 Immunological, paracrine and endocrine aspects of testicular immune privilege. *Molecular and Cellular Endocrinology* **335** 60–68. (doi:10.1016/j.mce.2010.03.022)

Miller DS, Bauer B & Hartz AM 2008 Modulation of P-glycoprotein at the blood–brain barrier: opportunities to improve central nervous system pharmacotherapy. *Pharmacological Reviews* **60** 196–209. (doi:10.1124/pr.107.07109)

Mizuno N, Niwa T, Yotsumoto Y & Sugiyama Y 2003 Impact of drug transporter studies on drug discovery and development. *Pharmacological Reviews* **55** 425–461. (doi:10.1124/pr.55.3.1)

Mruk DD & Cheng CY 2008 Delivering non-hormonal contraceptives to men: advances and obstacles. *Trends in Biotechnology* **26** 90–99. (doi:10.1016/j.tibtech.2007.10.009)

Mruk DD, Zhu LJ, Silvestrini B, Lee WM & Cheng CY 1997 Interactions of proteases and protease inhibitors in Sertoli–germ cell cocultures preceding the formation of specialized Sertoli–germ cell junctions *in vitro*. *Journal of Andrology* **18** 612–622.

Mruk DD, Siu MKY, Conway AM, Lee NPY, Lau ASN & Cheng CY 2003 Role of tissue inhibitor of metalloproteases-1 in junction dynamics in the testis. *Journal of Andrology* **24** 510–523.

Mruk DD, Wong CH, Silvestrini B & Cheng CY 2006 A male contraceptive targeting germ cell adhesion. *Nature Medicine* **12** 1323–1328. (doi:10.1038/nm1420)

Mruk DD, Silvestrini B & Cheng CY 2008 Anchoring junctions as drug targets: role in contraceptive development. *Pharmacological Reviews* **60** 146–180. (doi:10.1124/pr.107.07105)

O'Donnell L, Nicholls PK, O'Bryan MK, McLachlan RI & Stanton PG 2011 Spermiation. The process of sperm release. *Spermatogenesis* **1** 14–35. (doi:10.4161/spmg.1.1.14525)

Ohtsuki S, Takizawa T, Takanaga H, Hori S, Hosoya KI & Terasaki T 2004 Localization of organic anion transporting polypeptide 3 (oatp3) in mouse brain parenchymal and capillary endothelial cells. *Journal of Neurochemistry* **90** 743–749. (doi:10.1111/j.1471-4159.2004.02549.x)

Okanlawon A & Dym M 1996 Effect of chloroquine on the formation of tight junctions in cultured immature rat Sertoli cells. *Journal of Andrology* **17** 249–255.

Orth JM 1982 Proliferation of Sertoli cells in fetal and postnatal rats: a quantitative autoradiographic study. *Anatomical Record* **203** 485–492. (doi:10.1002/ar.1092030408)

Rochat B 2009 Importance of influx and efflux systems and xenobiotic metabolizing enzymes in intratumoral disposition of anticancer agents. *Current Cancer Drug Targets* **9** 652–674. (doi:10.2174/156800909789056999)

Setchell BP 2008 Blood–testis barrier, junctional and transport proteins and spermatogenesis. In *Molecular Mechanisms in Spermatogenesis*, pp 212–233. Ed. CY Cheng. Austin, TX: Landes Bioscience/Springer Science + Business Media, LLC.

Shen S & Zhang W 2010 ABC transporters and drug efflux at the blood–brain barrier. *Reviews in the Neurosciences* **21** 29–53. (doi:10.1515/REVNEURO.2010.21.1.29)

Siu MKY, Lee WM & Cheng CY 2003 The interplay of collagen IV, tumor necrosis factor-α, gelatinase B (matrix metalloprotease-9), and tissue inhibitor of metalloprotease-1 in the basal lamina regulates Sertoli cell-tight junction dynamics in the rat testis. *Endocrinology* **144** 371–387. (doi:10.1210/en.2002-220786)

Siu MKY, Wong CH, Lee WM & Cheng CY 2005 Sertoli–germ cell anchoring junction dynamics in the testis are regulated by an interplay of lipid and protein kinases. *Journal of Biological Chemistry* **280** 25029–25047. (doi:10.1074/jbc.M501049200)

Siu ER, Wong EWP, Mruk DD, Porto CS & Cheng CY 2009*a* Focal adhesion kinase is a blood–testis barrier regulator. *PNAS* **106** 9298–9303. (doi:10.1073/pnas.0813113106)

Siu ER, Wong EWP, Mruk DD, Sze KL, Porto CS & Cheng CY 2009*b* An occludin-focal adhesion kinase protein complex at the blood–testis barrier: a study using the cadmium model. *Endocrinology* **150** 3336–3344. (doi:10.1210/en.2008-1741)

Siu MKY, Wong CH, Xia W, Mruk DD, Lee WM & Cheng CY 2011 The β1-integrin-p-FAK-p130Cas-DOCK180-RhoA-vinculin is a novel regulatory protein complex at the apical ectoplasmic specialization in adult rat testes. *Spermatogenesis* **1** 73–86. (doi:10.4161/spmg.1.1.15452)

Su L, Cheng CY & Mruk DD 2009 Drug transporter, P-glycoprotein (MDR1), is an integrated component of the mammalian blood–testis barrier. *International Journal of Biochemistry and Cell Biology* **41** 2578–2587. (doi:10.1016/j.biocel.2009.08.015)

Su L, Cheng CY & Mruk DD 2010*a* Adjudin-mediated Sertoli–germ cell junction disassembly affects Sertoli cell barrier function *in vitro* and *in vivo*. *International Journal of Biochemistry and Cell Biology* **42** 1864–1875. (doi:10.1016/j.biocel.2010.08.004)

Su L, Mruk DD & Cheng CY 2010*b* Drug transporters, the blood–testis barrier, and spermatogenesis. *Journal of Endocrinology* **208** 207–223. (doi:10.1677/JOE-10-0363)

Su L, Mruk DD, Lee WM & Cheng CY 2010*c* Differential effects of testosterone and TGF-β3 on endocytic vesicle-mediated protein trafficking events at the blood–testis barrier. *Experimental Cell Research* **316** 2945–2960. (doi:10.1016/j.yexcr.2010.07.018)

Suzuki T, Onogawa T, Asano N, Mizutamari H, Mikkaichi T, Tanemoto M, Abe M, Satoh F, Unno M, Nunoki K *et al.* 2003 Identification and characterization of novel rat and human gonad-specific organic anion transporters. *Molecular Endocrinology* **17** 1203–1215. (doi:10.1210/me.2002-0304)

Ueno M, Nakagawa T, Wu B, Onodera M, Huang CL, Kusaka T, Araki N & Sakamoto H 2010 Transporters in the brain endothelial barrier. *Current Medicinal Chemistry* **17** 1125–1138. (doi:10.2174/092986710790827816)

Wong CH, Mruk DD, Lui WY & Cheng CY 2004 Regulation of blood–testis barrier dynamics: an *in vivo* study. *Journal of Cell Science* **117** 783–798. (doi:10.1242/jcs.00900)

Wong CH, Mruk DD, Siu MKY & Cheng CY 2005 Blood–testis barrier dynamics are regulated by α2-macroglobulin via the c-Jun N-terminal protein kinase pathway. *Endocrinology* **146** 1893–1908. (doi:10.1210/en.2004-1464)

Wong EWP, Mruk DD & Cheng CY 2008*a* Biology and regulation of ectoplasmic specialization, an atypical adherens junction type, in the testis. *Biochimica et Biophysica Acta* **1778** 692–708. (doi:10.1016/j.bbamem.2007.11.006)

Wong EWP, Mruk DD, Lee WM & Cheng CY 2008*b* Par3/Par6 polarity complex coordinates apical ectoplasmic specialization and blood–testis barrier restructuring during spermatogenesis. *PNAS* **105** 9657–9662. (doi:10.1016/j.bbamem.2007.11.006)

Xia W, Mruk DD, Lee WM & Cheng CY 2007 Unraveling the molecular targets pertinent to junction restructuring events during spermatogenesis using the Adjudin-induced germ cell depletion model. *Journal of Endocrinology* **192** 563–583. (doi:10.1677/JOE-06-0158)

Xia W, Wong EWP, Mruk DD & Cheng CY 2009 TGF-β3 and TNFα perturb blood–testis barrier (BTB) dynamics by accelerating the clathrin-mediated endocytosis of integral membrane proteins: a new concept of BTB regulation during spermatogenesis. *Developmental Biology* **327** 48–61. (doi:10.1016/j.ydbio.2008.11.028)

Yan HHN & Cheng CY 2006 Laminin α3 forms a complex with β3 and γ3 chains that serves as the ligand for α6β1-integrin at the apical ectoplasmic specialization in adult rat testes. *Journal of Biological Chemistry* **281** 17286–17303. (doi:10.1074/jbc.M513218200)

Yan HHN, Mruk DD, Lee WM & Cheng CY 2008*a* Blood–testis barrier dynamics are regulated by testosterone and cytokines via their differential effects on the kinetics of protein endocytosis and recycling in Sertoli cells. *FASEB Journal* **22** 1945–1959. (doi:10.1096/fj.06-070342)

Yan HHN, Mruk DD, Wong EWP, Lee WM & Cheng CY 2008*b* An autocrine axis in the testis that coordinates spermiation and blood–testis barrier restructuring during spermatogenesis. *PNAS* **105** 8950–8955. (doi:10.1073/pnas.0711264105)

Received in final form 5 March 2011
Accepted 6 April 2011
Made available online as an Accepted Preprint
6 April 2011